

Article

Thermo-Optical Generation of Particle-Like Structures in Frustrated Chiral Nematic Film

Sergey Shvetsov ^{1,2,*} , Tetiana Orlova ³ , Alexander V. Emelyanenko ¹ 
and Alexander Zolot'ko ²

¹ Faculty of Physics, Lomonosov Moscow State University, 119991 Moscow, Russia

² Lebedev Physical Institute, 119991 Moscow, Russia

³ Institut Charles Sadron, University of Strasbourg, CNRS, 67034 Strasbourg, France

* Correspondence: shvetsov@polly.phys.msu.ru

Received: 4 October 2019; Accepted: 28 October 2019; Published: 31 October 2019



Abstract: The creation of metastable particle-like structures in frustrated (unwound) chiral nematic film containing light-absorbing additive is studied. It is shown that such localized structures can be generated by the thermo-optical action of a focused laser beam or arise spontaneously at a phase transition from an isotropic to a liquid crystal state. Observed axisymmetric patterns resemble cholesteric spherulites with toroidal double-twisted director-field configuration.

Keywords: chiral nematic liquid crystal; azobenzene dye; light-matter interaction; phase transition; particle-like structure; optical memory; nonlinear optics

1. Introduction

Usually, the defects in solid crystals correspond to a violation of spatial location of ions or atoms in crystalline lattice. In contrast to ordinary crystals, the defects in liquid crystals are caused by uncertainty in the orientation of the director field, where the director indicates the average direction of the long axes of liquid crystal molecules. Liquid crystal defects can be optically visualized due to the far-field structures formed by them as a result of spatial elastic distortions of the director field.

Orientalional nature of liquid–crystalline defects manifests itself in points, lines, and walls with different topological configurations [1,2]. In chiral nematic or cholesteric liquid crystals (CLCs), which contain chiral molecules or consist of them, a diversity of orientational configurations can be realized [3–5]. Under certain conditions, the axisymmetric structures with complex internal structure known as cholesteric bubbles or spherulites may arise in unwound CLC films [6]. These structures possess a double-twisted director-field configuration looped into the torus.

Orientalional structure of a CLC film placed between two substrates, which provide homeotropic anchoring conditions, usually depends on the ratio between the film thickness L and cholesteric pitch p_0 (the distance at which the director rotates on the angle 2π along the helical axis in unperturbed CLC) [7,8]. At the ratio of $L/p_0 \ll 1$, the CLC is obviously indistinguishable from nematic. With a decrease in cholesteric pitch to $L/p_0 \simeq 1$, unwound cholesteric state becomes unstable and fingerprint texture is formed [9]. In the limit of infinitely strong boundary conditions, the critical ratio of L/p_0 for the appearance of fingerprint texture can be found from a simple expression $L/p_0 = K_3/2K_2$, where K_2 and K_3 are the twist and bend elastic constants, respectively [10,11]. The finger-like structures can be transformed into cholesteric bubbles under the action of the alternating current (AC) electric field applied to the LC cell [12,13]. The spherulitic domains can also be formed in a uniform homeotropic state due to electrohydrodynamic instability [14–17] or at cooling down from isotropic phase [18]. Moreover, it was shown that these structures possess some particle properties, i.e., there are repulsive and attractive interactions between them [15,16].

Of special interest is the optical generation of such localized patterns due to the possibility of spatial addressing that allows creating predefined arrays of the particle-like structures. The complex orientational domain can be induced by a unstructured (Gaussian) or structured (optical vortex) focused light beam [19–23] owing to the direct reorienting light action. In a number of comprehensive studies involving fluorescence confocal polarizing microscopy, different localized structures such as torons, skrymions and “finger loops” were generated [22]. Another approach lies in the generation of a particle-like structure in a photoactive CLC doped with photoresponsive chiral additive, when a focused light beam causes a decrease in the cholesteric pitch due to photochemical isomerization of dopant molecules [24,25]. Despite the various mechanisms of complex structure formation, it was shown that the electrically generated cholesteric bubbles possess the same orientational ordering as optically generated torons [17,21]. Toron-like structures can be also obtained in other spatially confined CLC systems, such as spherical shells [26], droplets [27–29], and microchannels [30], as well as in CLC films containing colloid particles [31].

Here, we present the thermo-optical generation of localized axisymmetric domains in frustrated CLC films doped with an azobenzene compound. The main idea is that the focused light beam causes the local heating, which leads to the formation of particle-like structures due to the distortions in the director field. This situation is compared with the generation of axisymmetric structures by a spatially uniform temperature variation throughout the CLC film.

2. Results

2.1. The Effect of Light Beam Exposure

The nonlinear optical response of CLC film (Sample 1) doped with 0.2 wt % of azobenzene dye (Methyl Red) was studied in comparison with a chiral nematic liquid crystal (NLC) containing the same 0.2 wt % of dye dopant (Sample 2). The initial alignment of LC films was the same and homeotropic in both samples. The samples were irradiated with a Gaussian light beam at normal incidence. The light wavelength of 532 nm lied within the dye absorption band. A detailed description of experimental setup and the samples under study is given in Section 4.

When the light beam power reached several milliwatts (the intensity on the light beam axis was about 10 W/cm^2), the light beam was broadened, and the “thermal” aberrational rings were formed in its cross-section (Figure 1(a1–a3,c1–c3)). The formation time of the aberrational pattern was about several milliseconds. This effect is caused by a decrease in order parameter due to the local heating under light beam exposure [32]. At the same time, we observed the nonzero intensity of light transmitted through the crossed polarizer at local heating of the CLC film (Figure 1(b1–b3)), whereas the polarization state of light passed through the NLC sample remained the same (Figure 1(d1–d3)). This indicates the appearance of director field distortions in the frustrated orientational structure of CLC film. The cross-like pattern (Figure 1(b2,b3)) can be attributed to the axially symmetric director distortion due to a thermo-mechanical effect in frustrated CLC film theoretically predicted in the study [33]. Importantly, the light broadening and the director field distortions were reversible in the samples, when the beam power was increased up to $P = 3.1 \text{ mW}$ and $P = 3.5 \text{ mW}$ for CLC and NLC, respectively.

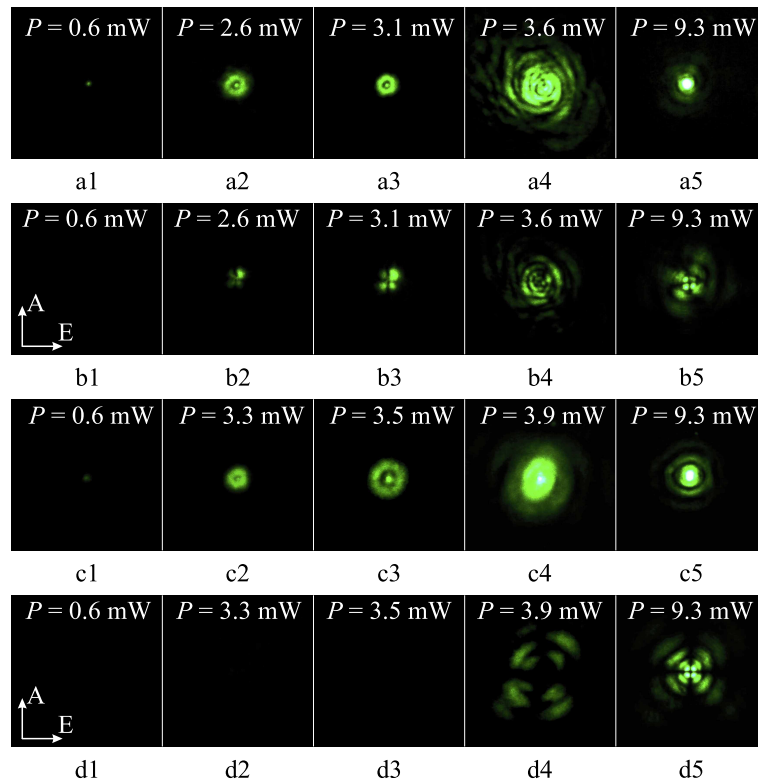


Figure 1. Far-field intensity distributions of the light beam passed through the homeotropically aligned films of 5CB + 0.2%MR + 0.025%BA (**a,b**) and 5CB + 0.2%MR (**c,d**) at different power P of incident light beam. Images (**b,d**) were obtained under cross-polarization conditions, when the transmission direction of the analyzer (A) placed after the sample was crossed with the direction of the electric field (E) in the incident light beam. The angular size of pictures equals 0.13 rad.

A further growth in the light beam power led to an abrupt increase in the light beam divergence (Figure 1(a4,c4)) due to the formation of an isotropic region that resulted in the axially symmetric reorientation of a director field in the vicinity of this region [34]. In the nematic sample, a cross-like pattern similar to a conoscopic picture was observed at the light transmission through the crossed polarizer (Figure 1(d4)). Such intensity distribution usually corresponds to a radial deformation of director field. This type of a light-beam self-action has already been used for optical vortex generation caused by light interaction with dye-doped nematic film [35]. In the cholesteric sample, the light intensity distribution obtained at the locally induced phase transition is more complex (Figure 1(b4)) than that for NLC film, but, with a further increase in the beam power, the intensity distributions in the case of nematic and cholesteric samples become similar (Figure 1(b5,d5)).

Once the isotropic region was formed in CLC film under the action of a light beam (corresponds to Figure 1(b4,b5)), a further decrease in the light beam power to $P = 0.6$ mW led to a strong beam divergence accompanied by formation of a ring-shaped diffraction pattern within several tens of seconds (Figure 2a). In contrast to this, a homogenous homeotropic orientation is restored in the NLC film after an isotropic-nematic transition.

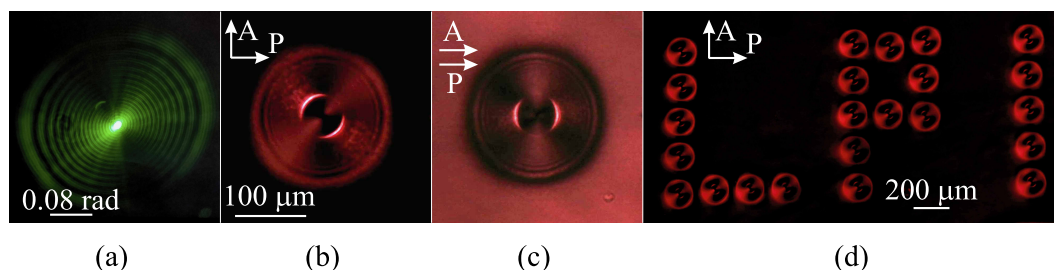


Figure 2. Far-field diffraction pattern of a probe light beam passed through the light-induced orientational structure created in the homeotropic film of 5CB + 0.2%MR + 0.02%BA (a). Optical microscopic images of this structure in the case of crossed (b) and parallel (c) polarizers. An example of addressed laser writing of the “LPI” pattern consisting of particle-like structures (d). White arrows in (b–d) indicate the directions of polarizer (P) and analyzer (A).

The illuminated area in the CLC sample was examined by polarized optical microscopy in the case of crossed (Figure 2b) and parallel (Figure 2c) polarizers. The microscopic images of light-induced domain remained unchanged at the microscope table rotation, which indicates the axisymmetric distribution of the director field inside it. The obtained particle-like structure remains stable for at least four weeks. Such generation method of localized orientational domains allows one to obtain the predefined composite pattern by spatially addressed writing (Figure 2d).

Note that an increase in the light beam waist w_0 up to three times at the sample shifting out of the light beam focus along the optical axis results in the formation of the same particle-like structure. In the case of an increase in the light beam power of about five times, an isotropic area becomes larger in size, which results in several particle-like structures appearing.

2.2. The Effect of Uniform Thermal and AC Electric Fields

To verify the thermal origin of axisymmetric structures, we have investigated the temperature effect in LC films. To this end, the CLC film (Sample 1) was uniformly heated to 35 °C that corresponds to the nematic-to-isotropic phase transition for the undoped NLC and then cooled to room temperature with the rate 0.1 °C/min. During the cooling process, the dense packed domains with the axisymmetric orientational structure appeared spontaneously (Figure 3a). These particle-like structures, as well as light-generated ones, were long-living at room temperature. Since similar orientational domains are formed in Sample 1 under the action of light beam, we assume the same thermal origin of the particle-like structures in both creation methods.

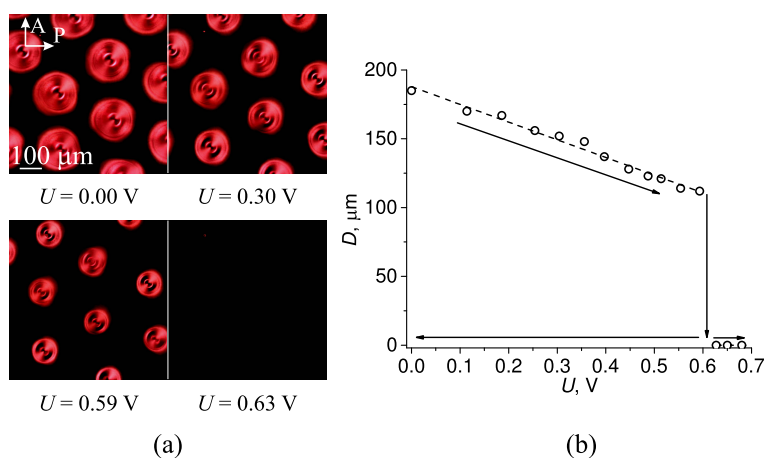


Figure 3. The particle-like structures formed during cooling from isotropic phase and the effect of applied electric field on the size of the axisymmetric structures (a); the dependence of the structure diameter D on the electric field voltage V (b).

Let us now consider the influence of electric field applied to the LC cell. Due to the positive dielectric anisotropy of 5CB liquid crystal, the electric field tends to rotate the director perpendicularly to the substrates, restoring the homeotropic anchoring of LC molecules. Indeed, we observed the reduction of the structure diameter with an increase in the applied voltage (Figure 3). Each data point was measured after at least 20 min after changing the electric field voltage to ensure the equilibrium state of a structure. It is interesting to note that this plot is well approximated by linear dependence. At the certain critical value $U_{cr} = 0.63$ V, the particle-like structures became unstable: their size was continuously reduced until they finally disappeared. No localized orientational domains or any other director field distortions were restored upon a subsequent voltage decrease. The same structural evolution under an AC electric field was observed in the case of thermo-optically generated domains.

3. Discussion

Summarizing the results obtained, we conclude that particle-like structures formed in the frustrated CLC under the focused beam exposure are originated from a light-induced phase transition. Our estimations show that the calculated threshold power of the light beam necessary for inducing the liquid crystal–isotropic phase transition is close to the experimental values under the assumption of heating caused by the absorption of light by the azobenzene dye (see Appendix A). The photoinduced cis-isomers of azobenzene dye molecules can additionally reduce the isotropization temperature; however, in this particular case, the effect of their presence is negligible due to low dye concentration 0.2 wt.%.

Here, we note that, at $K_1 - 3(K_3 - K_2) < 0$ (K_i are splay, twist, and bend elastic constants), a coexisting deformed state should exist below the critical ratio L/p_0 [10,11]. This inequality is satisfied for elastic constants in the temperature range of the 5CB mesophase [36], a basic material of a CLC sample. In other words, if the director deformation overcomes some critical value, the director field does not relax to a homogeneous state. We assume that this value is reached when an isotropic channel is formed, based on the fact that the polar angle of the director reaches $\approx 65^\circ$ at an LC–isotropic interface [37,38]. We believe that these distortions of the director field are large enough to allow the formation of a metastable liquid crystal state upon gradual cooling of the isotropic area. The particle-like structure possesses a twisted director configuration formed due to the symmetry reason and interplay between chirality of CLC, its elasticity, anchoring conditions, and confinement.

The optical images of the generated axisymmetric structure resemble those taken for bubble domain [6] or toron [19]. The observed light diffraction pattern (Figure 2a) is also similar to the patterns, obtained upon light propagation through a cholesteric bubble [14,39,40]. Based on this, we believe that thermo-optically induced domains possess a director field distribution similar to that of bubble domains [13].

The suppression of the light-induced domain in electric field confirms the bulk origin of director reorientation, thus we conclude that no bulk-mediated photoalignment effect [41] occurs in our case. At the same time, azobenzene dopants are known to cause director reorientation in a bulk of liquid crystal [42]. As this effect can contribute to the director field distortion, perhaps it is the reason for a more pronounced far-field intensity distribution at higher light beam power (Figure 1(a5,d5)). Our observation of the evolution of the cholesteric bubble diameter with an applied electric field is in good qualitative agreement with already reported experimental data obtained for various values of the confinement ratio L/p_0 [13].

Another factor which may affect the formation of particle-like structure is a change in the cholesteric pitch p_0 at temperature variation. To analyze this possibility, we studied a sample of 5CB liquid crystal doped with higher concentration of chiral dopant (Sample 3). We found that p_0 decreases from 3.7 μm to 3.6 μm during the temperature rise up to the phase transition, i.e., the relative variation in cholesteric pitch value is less than 3%. Based on this, we assume that, in the case of Sample 1, with the same chiral dopant, the change in the cholesteric pitch p_0 caused by temperature is also small and cannot be the reason for the formation of an orientational domain.

The appearance of a number of particle-like structures with a spatially uniform temperature variation throughout the CLC film is most likely associated with the formation of many isotropic droplets in the LC phase upon cooling. Unlike spatially-addressed light-induced structures, these spherulite domains appear spontaneously and form a dense packed composite pattern.

In general, our experimental findings demonstrate a simple thermo-optical approach for addressed generation of localized twisted structures in a uniformly unwound CLC using a focused light beam with a low power level of the order of several milliwatts. Our approach compares favorably with the previously proposed optically triggered generation of localized structures in CLC films by supramolecular reorientation that requires at least 30–50 mW power budget to create a single structure [19]. Opto-molecular generation of particle-like structures in photoactive CLCs at an extremely low nanowatt power level has been shown [24]; however, the formed twisted structures were unstable in time after the interruption of the laser beam irradiation and relaxed to the initial unwound CLC state [24,25]. The addressed creation of defect structures in an unwound CLC film using electric field requires a patterned electrode design [43], otherwise localized structures appear randomly [13], similar to the cooling process from an isotropic LC state.

4. Materials and Methods

4.1. Sample Preparation

The cholesteric liquid-crystalline (LC) mixture (Sample 1) was composed of 5CB nematic liquid crystal, 0.025 wt % of chiral dopant Benzoic Acid (BA), 4-(trans-4-pentylcyclohexyl)-1,1'-[(1(S(+)))-1-phenyl-1,2-ethanediyl] ester (Synthon Chemicals), and 0.2 wt % of Methyl Red azobenzene dye (Aldrich). The nematic LC mixture (Sample 2) was composed of 5CB liquid crystal doped with 0.2 wt % of Methyl Red azobenzene dye (Aldrich). To prepare the LC mixtures, the compounds were dissolved and mixed in chloroform with subsequent evaporation of the solvent. The cholesteric pitch for the Sample 1 measured by the Grandjean–Cano method was $p_0 = 113 \mu\text{m}$.

We assume that the elastic constants of Sample 1 are close to those of 5CB liquid crystal due to low dopant concentrations. According to the study [36], the constants of splay, twist, and bend deformations are equal to $K_1 = 6.2 \text{ pN}$, $K_2 = 3.8 \text{ pN}$, $K_3 = 8.5 \text{ pN}$ at $T = 25 \text{ }^\circ\text{C}$ and $K_1 = 2.4 \text{ pN}$, $K_2 = 1.3 \text{ pN}$, $K_3 = 2.9 \text{ pN}$ at $T = 34.5 \text{ }^\circ\text{C}$.

The LC cells were made of two glass substrates with indium tin oxide (ITO) coating. For homeotropic anchoring conditions, the glass substrates were treated by chromium stearyl chloride with a subsequent annealing for 1 h at $95 \text{ }^\circ\text{C}$. The substrates were separated by teflon spacers, so that the cell thickness was $L = 86 \pm 2 \mu\text{m}$ ($L/p_0 = 0.76$). The absorption coefficients of Sample 1 and Sample 2 at the wavelength $\lambda = 532 \text{ nm}$ were measured using MC-122 spectrophotometer (Proscan Special Instruments, Belarus) and equals $\alpha_1 = 213 \text{ cm}^{-1}$ and $\alpha_2 = 225 \text{ cm}^{-1}$, respectively.

The critical thickness, at which finger-like cholesteric structures appear in Sample 1, is $L_{cr} \approx 99 \mu\text{m}$ (or, $L_{cr}/p_0 = 0.88$). It was determined by using a wedge LC cell with homeotropic anchoring conditions (the wedge angle is $\gamma = 5.5 \cdot 10^{-3} \text{ rad}$).

The investigation of $p_0(T)$ dependence was performed for 5CB nematic liquid crystal doped with 0.4 wt % of BA in a wedge cell with polyimide treated substrates providing planar anchoring conditions (Sample 3).

4.2. Optical Setup

The light beam from a continuous-wave solid-state laser (Integrated Optics) with the wavelength $\lambda = 532 \text{ nm}$ and linear (horizontal) polarization (E) passed through a neutral density filter and was focused on the sample at normal incidence conditions. The beam waist radius was measured to be $w_0 = 71 \pm 2 \mu\text{m}$ at the intensity level of $1/e^2$. In some measurements, the analyzing polarizer (A) with vertical propagation direction was installed after the sample. Far field diffraction patterns formed on a

semi-transparent screen behind the sample were recorded by a USB-camera. The experiments were carried out at room temperature ($T = 24\text{--}26\text{ }^{\circ}\text{C}$).

4.3. Optical Microscopy

Polarized optical microscopy was carried out using an Eclipse LV100N Pol microscope (Nikon, Japan) equipped with a heating stage (Linkam Scientific, United Kingdom) and a USB camera. To avoid the influence of backlight illumination from the built-in halogen lamp, a ZhS-17 yellow filter was used.

A sinusoidal electric field from a signal generator with a frequency of $f = 1\text{ kHz}$ was applied to ITO-coated cell substrates, when necessary.

5. Conclusions

We have studied the light-induced generation of axisymmetric particle-like structures in an unwound CLC doped with the light-absorbing dye. It is shown that such structures can be generated by local heating under the action of a focused light beam, which leads to the formation of a local isotropic region and, as a result, to the orientation distortion in the initially uniform homeotropic film. The cooling of this region in the presence of the orientation distortions leads to the formation of an axisymmetric domain with twisted director field configuration.

A spatially addressed writing of predefined composite patterns consisting of a number of particle-like structures is also demonstrated. A similar pattern, but without a predefined spatial distribution of particle-like structures, can appear spontaneously when the entire sample is cooled from an isotropic state. The size of particle-like structures can be controlled by an AC electric field. In comparison with previously described generation methods of particle-like metastable structures, the main advantage is the possibility of metastable structure formation under the local action low-intensity light beams.

The main advantage of the thermo-optical approach is the on-demand generation of localized particle-like structures by a light beam with a power level of only a few milliwatts. The formed twisted domains remain stable for at least several weeks after the interruption of the light beam expose. The presented method can find its application in the development of tunable optical elements for photonics applications, such as micro-lenses [39] and beam mode converters [44].

Author Contributions: Conceptualization, S.S., T.O. and A.Z.; investigation, S.S.; writing—original draft preparation, S.S. and T.O.; supervision, A.V.E. and A.Z.

Funding: This research was funded by Russian Science Foundation, Grant No. 18-72-00242.

Acknowledgments: S.S. is grateful to Anatoly V. Kaznacheev for fruitful discussions.

Conflicts of Interest: The authors declare no conflict of interest.

Abbreviations

The following abbreviations are used in this manuscript:

CLC	Cholesteric liquid crystal
NLC	Nematic liquid crystal
LC	Liquid crystalline
BA	Benzoic Acid
ITO	Indium tin oxide

Appendix A

Let us estimate the optical threshold power P_{th} required for the heating an absorbing liquid crystalline mixture from an ambient temperature T to the nematic–isotropic transition point $T_{NI} = 35\text{ }^{\circ}\text{C}$. According to [45], for the Gaussian beam, this threshold can be calculated as follows:

$$P_{th} = \frac{2\pi\kappa_{\perp}w(T_{NI} - T)}{Af(w/L)}, \quad (A1)$$

where $A = 1 - \exp(-\alpha_{\perp}L)$, $w = w_0/\sqrt{2}$, κ_{\perp} is the perpendicular component of the heat conductivity tensor, and $f(w/L)$ is a function calculated in the study [45]. Under our experimental conditions, the ratio of w/L equals 0.58, and the corresponding value $f(w/L)$ is 0.23 (according to [45]). At the ambient temperature $T = 25$ °C, κ_{\perp} equals 1.3 mW/(cm·°C) [46]. In this case, Equation (1) yields $P_{th} = 2.1$ mW.

This value is somewhat smaller than the obtained experimental values $P_{th} = 3.1$ mW and $P_{th} = 3.5$ mW for CLC and NLC, respectively, that we obtained. However, the calculation according to the model presented in [45] gives us a reasonable result. The difference with experiments may be due to several reasons. One of them is the light-induced conversion of trans-isomers to the metastable cis-form that may cause a decrease in the absorption coefficient of the LC film. Another reason is an increase in the absorption of trans-isomers in LC matrix owing to decreasing their order parameter with temperature increase.

References

1. Kurik, M.V.; Lavrentovich, O.D. Defects in liquid crystals: homotopy theory and experimental studies. *Sov. Phys. Uspekhi* **1988**, *31*, 196–224, doi:10.1070/PU1988v031n03ABEH005710. [CrossRef]
2. Kleman, M.; Lavrentovich, O.D. Topological point defects in nematic liquid crystals. *Philos. Mag.* **2006**, *86*, 4117–4137, doi:10.1080/14786430600593016. [CrossRef]
3. Nych, A.; Ognysta, U.; Mušević, I.; Seč, D.; Ravnik, M.; Žumer, S. Chiral bipolar colloids from nonchiral chromonic liquid crystals. *Phys. Rev. E* **2014**, *89*, 062502, doi:10.1103/PhysRevE.89.062502. [CrossRef]
4. Ackerman, P.J.; Smalyukh, I.I. Diversity of Knot Solitons in Liquid Crystals Manifested by Linking of Preimages in Torons and Hopfions. *Phys. Rev. X* **2017**, *7*, 011006, doi:10.1103/PhysRevX.7.011006. [CrossRef]
5. Orlova, T.; Ašhoff, S.J.; Yamaguchi, T.; Katsonis, N.; Brasselet, E. Creation and manipulation of topological states in chiral nematic microspheres. *Nat. Commun.* **2015**, *6*, 7603, doi:10.1038/ncomms8603. [CrossRef]
6. Oswald, P.; Pieranski, P. *Nematic and Cholesteric Liquid Crystals*; CRC Press: Boca Raton, FL, USA, 2005; doi:10.1201/9780203023013. [CrossRef]
7. Oswald, P.; Baudry, J.; Pirkel, S. Static and dynamic properties of cholesteric fingers in electric field. *Phys. Rep.* **2000**, *337*, 67–96, doi:10.1016/S0370-1573(00)00056-9. [CrossRef]
8. Smalyukh, I.I.; Senyuk, B.I.; Palfy-Muhoray, P.; Lavrentovich, O.D.; Huang, H.; Gartland, E.C.; Bodnar, V.H.; Kosa, T.; Taheri, B. Electric-field-induced nematic-cholesteric transition and three-dimensional director structures in homeotropic cells. *Phys. Rev. E* **2005**, *72*, 061707, doi:10.1103/PhysRevE.72.061707. [CrossRef]
9. Dierking, I. *Textures of Liquid Crystals*; Wiley-VCH: Hoboken, NJ, USA, 2003; doi:10.1002/3527602054. [CrossRef]
10. Zeldovich, B.; Tabiryan, N. Freedericksz transition in cholesteric liquid-crystals without external fields. *JETP Lett.* **1981**, *34*, 406–408.
11. Tabiryan, N.V.; Zeldovich, B.Y. Equilibrium structure of a cholesteric with homeotropic orientation on the walls. *J. Exp. Theor. Phys.* **1982**, *56*, 563–566.
12. Nawa, N.; Nakamura, K. Observation of Forming Process of Bubble Domain Texture in Liquid Crystals. *Jpn. J. Appl. Phys.* **1978**, *17*, 219–225, doi:10.1143/jjap.17.219. [CrossRef]
13. Pirkel, S.; Ribière, P.; Oswald, P. Forming process and stability of bubble domains in dielectrically positive cholesteric liquid crystals. *Liq. Cryst.* **1993**, *13*, 413–425, doi:10.1080/02678299308026314. [CrossRef]
14. Bhide, V.G.; Chandra, S.; Jain, S.C.; Medhekar, R.K. Structure and properties of bubble domains in cholesteric-nematic mixtures. *J. Appl. Phys.* **1976**, *47*, 120–126, doi:10.1063/1.322305. [CrossRef]
15. Gilli, J.M.; Thiberge, S.; Manaila-Maximean, D. New Aspect of the Voltage/Confinement Ratio Phase Diagram for a Confined Homeotropic Cholesteric. *Mol. Cryst. Liq. Cryst.* **2004**, *417*, 207–213, doi:10.1080/15421400490478858. [CrossRef]
16. Ackerman, P.J.; van de Lagemaat, J.; Smalyukh, I.I. Self-assembly and electrostriction of arrays and chains of hopfion particles in chiral liquid crystals. *Nat. Commun.* **2015**, *6*, 6012, doi:10.1038/ncomms7012. [CrossRef]

17. Varanytsia, A.; Posnjak, G.; Mur, U.; Joshi, V.; Darrah, K.; Mušević, I.; Čopar, S.; Chien, L.C. Topology-commanded optical properties of bistable electric-field-induced torons in cholesteric bubble domains. *Sci. Rep.* **2017**, *7*, 16149, doi:10.1038/s41598-017-16241-4. [[CrossRef](#)]
18. Carboni, C.; Al-Lawati, A.; George, A.K.; Al-Harhi, S.H.; Al-Barwani, M. Observation of a Bubble Texture At the Cholesteric To Homeotropic-Nematic Transition In a Confined Chiral Nematic Liquid Crystal. *Mol. Cryst. Liq. Cryst.* **2004**, *410*, 239–245, doi:10.1080/15421400490436043. [[CrossRef](#)]
19. Smalyukh, I.I.; Lansac, Y.; Clark, N.A.; Trivedi, R.P. Three-dimensional structure and multistable optical switching of triple-twisted particle-like excitations in anisotropic fluids. *Nat. Mater.* **2010**, *9*, 139–145, doi:10.1038/nmat2592. [[CrossRef](#)]
20. Smalyukh, I.I.; Kaputa, D.; Kachynski, A.V.; Kuzmin, A.N.; Ackerman, P.J.; Twombly, C.W.; Lee, T.; Trivedi, R.P.; Prasad, P.N. Optically generated reconfigurable photonic structures of elastic quasiparticles in frustrated cholesteric liquid crystals. *Opt. Express* **2012**, *20*, 6870, doi:10.1364/OE.20.006870. [[CrossRef](#)]
21. Ackerman, P.J.; Qi, Z.; Smalyukh, I.I. Optical generation of crystalline, quasicrystalline, and arbitrary arrays of torons in confined cholesteric liquid crystals for patterning of optical vortices in laser beams. *Phys. Rev. E* **2012**, *86*, 021703, doi:10.1103/PhysRevE.86.021703. [[CrossRef](#)]
22. Ackerman, P.J.; Trivedi, R.P.; Senyuk, B.; van de Lagemaat, J.; Smalyukh, I.I. Two-dimensional skyrmions and other solitonic structures in confinement-frustrated chiral nematics. *Phys. Rev. E* **2014**, *90*, 012505, doi:10.1103/PhysRevE.90.012505. [[CrossRef](#)]
23. Loussert, C.; Brasselet, E. Multiple chiral topological states in liquid crystals from unstructured light beams. *Appl. Phys. Lett.* **2014**, *104*, 051911, doi:10.1063/1.4864096. [[CrossRef](#)]
24. Loussert, C.; Iamsaard, S.; Katsonis, N.; Brasselet, E. Subnanowatt Opto-Molecular Generation of Localized Defects in Chiral Liquid Crystals. *Adv. Mater.* **2014**, *26*, 4242–4246, doi:10.1002/adma.201400811. [[CrossRef](#)]
25. Orlova, T.; Lancia, F.; Loussert, C.; Iamsaard, S.; Katsonis, N.; Brasselet, E. Revolving supramolecular chiral structures powered by light in nanomotor-doped liquid crystals. *Nat. Nanotechnol.* **2018**, *13*, 304–308, doi:10.1038/s41565-017-0059-x. [[CrossRef](#)]
26. Darmon, A.; Benzaquen, M.; Seč, D.; Čopar, S.; Dauchot, O.; Lopez-Leon, T. Waltzing route toward double-helix formation in cholesteric shells. *Proc. Natl. Acad. Sci. USA* **2016**, *113*, 9469–9474, doi:10.1073/pnas.1525059113. [[CrossRef](#)]
27. Krakhalev, M.N.; Rudyak, V.Y.; Gardymova, A.P.; Zyryanov, V.Y. Toroidal Configuration of a Cholesteric Liquid Crystal in Droplets with Homeotropic Anchoring. *JETP Lett.* **2019**, *109*, 478–481, doi:10.1134/S0021364019070075. [[CrossRef](#)]
28. Krakhalev, M.N.; Rudyak, V.Y.; Prishchepa, O.O.; Gardymova, A.P.; Emelyanenko, A.V.; Liu, J.H.; Zyryanov, V.Y. Orientational structures in cholesteric droplets with homeotropic surface anchoring. *Soft Matter* **2019**, *15*, 5554–5561, doi:10.1039/C9SM00384C. [[CrossRef](#)]
29. Posnjak, G.; Čopar, S.; Mušević, I. Points, skyrmions and torons in chiral nematic droplets. *Sci. Rep.* **2016**, *6*, 26361, doi:10.1038/srep26361. [[CrossRef](#)]
30. Kim, Y.H.; Gim, M.J.; Jung, H.T.; Yoon, D.K. Periodic arrays of liquid crystalline torons in microchannels. *RSC Adv.* **2015**, *5*, 19279–19283, doi:10.1039/C4RA16883F. [[CrossRef](#)]
31. Pandey, M.B.; Ackerman, P.J.; Burkart, A.; Porenta, T.; Žumer, S.; Smalyukh, I.I. Topology and self-assembly of defect-colloidal superstructure in confined chiral nematic liquid crystals. *Phys. Rev. E* **2015**, *91*, 012501, doi:10.1103/PhysRevE.91.012501. [[CrossRef](#)]
32. Volterra, V.; Wiener-Avneer, E. Cw thermal lens effect in thin layer of nematic liquid crystal. *Opt. Commun.* **1974**, *12*, 194–197, doi:10.1016/0030-4018(74)90389-7. [[CrossRef](#)]
33. Zeldovich, B.Y.; Akopyan, R. Thermomechanical effects in deformed nematics. *J. Exp. Theor. Phys.* **1984**, *60*, 953–958.
34. Barnik, M.I.; Zolot'ko, A.S.; Kitaeva, V.F. Interaction of light with a dye-doped nematic liquid crystal. *J. Exp. Theor. Phys.* **1997**, *84*, 1122–1130, doi:10.1134/1.558249. [[CrossRef](#)]
35. Budagovsky, I.A.; Zolot'ko, A.S.; Korshunov, D.L.; Smayev, M.P.; Shvetsov, S.A.; Barnik, M.I. Generation of spiral dislocation of wave front in absorbing nematic liquid crystal. *Opt. Spectrosc.* **2015**, *119*, 280–285, doi:10.1134/s0030400x15080044. [[CrossRef](#)]
36. Cui, M.; Kelly, J.R. Temperature Dependence of Visco-Elastic Properties of 5CB. *Mol. Cryst. Liq. Cryst. Sci. Technol. Sec. A Mol. Cryst. Liq. Cryst.* **1999**, *331*, 49–57, doi:10.1080/10587259908047499. [[CrossRef](#)]

37. Faetti, S.; Palleschi, V. Nematic-isotropic interface of some members of the homologous series of 4-cyano-4'-(n-alkyl)biphenyl liquid crystals. *Phys. Rev. A* **1984**, *30*, 3241–3251, doi:10.1103/PhysRevA.30.3241. [[CrossRef](#)]
38. Holyst, R.; Poniewierski, A. Orientation of Liquid-Crystal Molecules at the Nematic-Isotropic Interface and the Nematic Free Surface. *Mol. Cryst. Liq. Cryst. Inc. Nonlinear Opt.* **1990**, *192*, 65–67, doi:10.1080/00268949008035607. [[CrossRef](#)]
39. Hamdi, R.; Petriashvili, G.; Lombardo, G.; De Santo, M.P.; Barberi, R. Liquid crystal bubbles forming a tunable micro-lenses array. *J. Appl. Phys.* **2011**, *110*, 074902, doi:10.1063/1.3642972. [[CrossRef](#)]
40. Haas, W.E.L.; Adams, J.E. Electrically variable diffraction in spherulitic liquid crystals. *Appl. Phys. Lett.* **1974**, *25*, 263–264, doi:10.1063/1.1655464. [[CrossRef](#)]
41. Yaroshchuk, O.; Reznikov, Y. Photoalignment of liquid crystals: basics and current trends. *J. Mater. Chem.* **2012**, *22*, 286–300, doi:10.1039/c1jm13485j. [[CrossRef](#)]
42. Janossy, I.; Lloyd, A.D. Low-Power Optical Reorientation in Dyed Nematics. *Mol. Cryst. Liq. Cryst.* **1991**, *203*, 77–84, doi:10.1080/00268949108046047. [[CrossRef](#)]
43. Loussert, C.; Kushnir, K.; Brasselet, E. Q-plates micro-arrays for parallel processing of the photon orbital angular momentum. *Appl. Phys. Lett.* **2014**, *105*, 121108, doi:10.1063/1.4895706. [[CrossRef](#)]
44. Yang, B.; Brasselet, E. Arbitrary vortex arrays realized from optical winding of frustrated chiral liquid crystals. *J. Opt.* **2013**, *15*, 044021, doi:10.1088/2040-8978/15/4/044021. [[CrossRef](#)]
45. Janossy, I.; Kosa, T. Laser-Induced Effects in Dyed Nematics. *Mol. Cryst. Liq. Cryst.* **1991**, *207*, 189–197. [[CrossRef](#)]
46. Ahlers, G.; Cannell, D.S.; Berge, L.I.; Sakurai, S. Thermal conductivity of the nematic liquid crystal 4-n-pentyl-4'-cyanobiphenyl. *Phys. Rev. E* **1994**, *49*, 545–553, doi:10.1103/PhysRevE.49.545. [[CrossRef](#)] [[PubMed](#)]



© 2019 by the authors. Licensee MDPI, Basel, Switzerland. This article is an open access article distributed under the terms and conditions of the Creative Commons Attribution (CC BY) license (<http://creativecommons.org/licenses/by/4.0/>).